

# Prompt $J/\psi$ production in hadronic $Z^0$ decays

OPAL Collaboration

## Abstract

Evidence for the production of prompt  $J/\psi$  mesons (not originating in b-hadron decays) in hadronic  $Z^0$  decays is presented. Using a sample of 3.6 million hadronic events, 24 prompt  $J/\psi$  candidates are identified from their decays into  $e^+e^-$  and  $\mu^+\mu^-$  pairs. The background is estimated to be  $10.8 \pm 1.8$  events. The following branching ratio for prompt  $J/\psi$  production is obtained:

$$Br(Z^0 \rightarrow \text{prompt } J/\psi + X) = (1.8 \pm 0.7 \pm 0.5 \pm 0.5) \cdot 10^{-4},$$

where the first error is statistical, the second systematic and the third error accounts for uncertainties in the prompt  $J/\psi$  production mechanism.

**Disclaimer:** The data presented in this Physics Note are **PRELIMINARY**. This note is only for the use of members of the OPAL collaboration and other persons who have been given explicit consent by OPAL.

# 1 Introduction

$J/\psi$  mesons are produced at LEP predominantly via b-hadron decays (see Fig. 1) with a measured branching ratio  $Br(Z^0 \rightarrow J/\psi + X)$  of about  $4.0 \cdot 10^{-3}$  [1–4]. A small number of  $J/\psi$  mesons, and other quarkonium states in general, are expected to be produced in fragmentation processes. The production of  $\Upsilon$  mesons in hadronic  $Z^0$  decays has already been observed [5], but at present only upper limits exist for prompt  $J/\psi$  production [6]. Recent interest in this prompt production mechanism is motivated by the observation at the Tevatron of quarkonium production rates larger than expected, and the subsequent attempt to explain the excess by the novel ‘colour-octet’ production models [7–9]. The production of prompt  $J/\psi$  in  $Z^0$  decays allows a non-trivial test of these models.

Initially, only ‘colour-singlet’ models were considered in estimating the production of prompt  $J/\psi$  mesons. In  $Z^0$  decays, these ‘colour-singlet’ fragmentation processes consist of ‘c-quark fragmentation’ [10], ‘gluon fragmentation’ [11] and ‘gluon radiation’ [12] contributions (see Fig. 2). The corresponding production rates have been calculated using perturbative QCD. According to these calculations [13], the ‘c-quark fragmentation’ process is dominant, with a branching ratio of:

$$Br(Z^0 \rightarrow J/\psi c\bar{c}) = 0.8 \cdot 10^{-4},$$

including the contribution of cascade decays from  $\psi'$  and  $\chi_c$  states. In the alternative ‘colour-octet’ models,  $J/\psi$  mesons are first produced in a ‘colour-octet’ state and then evolve non-perturbatively into ‘colour-singlet’ states by emission of soft gluons. According to [13], the dominant process in this case is the ‘gluon fragmentation’ process (see Fig. 2), with a branching ratio of:

$$Br(Z^0 \rightarrow J/\psi q\bar{q}) = 1.9 \cdot 10^{-4},$$

including cascade decays (see also alternative calculations in [14]). Both the colour-singlet and colour-octet QCD calculations suffer however from potentially large uncertainties since they include only leading terms. In the case of ‘colour-octet’ models, the total rate depends, in addition, on free parameters adjusted to the Tevatron data. The validity of these production models and rates has yet to be confirmed by experimental measurements.

In this paper, a search for prompt  $J/\psi$  mesons in  $Z^0$  decays is performed.  $J/\psi$  mesons are identified from their decays into  $e^+e^-$  and  $\mu^+\mu^-$  pairs. The outline of this paper is as follows: a brief description of the OPAL detector is presented in Section 2, the main  $J/\psi$  selection criteria are described in Section 3, the prompt  $J/\psi$  selection criteria are discussed in Section 4, and finally, the  $Z^0 \rightarrow$  prompt  $J/\psi + X$  branching ratio is obtained in Section 5.

## 2 The OPAL Detector

The OPAL detector has been described elsewhere [15]. The analysis presented here is based on information from the central tracking system, the lead glass electromagnetic calorimeter and its presampler, the hadron calorimeter and the muon chambers. The tracking system consists of a two layer silicon microstrip vertex detector [16], a vertex drift chamber, a jet chamber and a set of  $z$ -chambers for measurements in the  $z$  direction ( $z$  is the coordinate parallel to the beam axis), all enclosed by a solenoidal magnet coil which produces an axial field of 0.435 T. The main tracking detector is the jet chamber, which has a length of 4 m, a diameter of 3.7 m and which provides up to 159 space points and close to 100% track-finding efficiency for charged tracks in the region  $|\cos\theta| < 0.92$ , where  $\theta$  is the polar angle with respect to the electron beam direction. The momentum resolution in the  $x - y$  plane can be parametrised as  $(\sigma_{p_t}/p_t)^2 = (0.02)^2 + (0.0015 \cdot p_t)^2$ , with  $p_t$  in GeV/ $c$ . The jet chamber is also able to perform particle identification by energy loss ( $dE/dx$ ) measurements with a resolution of 3.5% for minimum ionising particles with the maximum number of ionisation samples [17].

### 3 Event samples and $J/\psi$ selection

The initial event sample consisted of hadronic  $Z^0$  decays recorded by OPAL in 1990-94 and selected using standard criteria [18]. Tracks were required to satisfy minimum quality cuts as in [19] and only events with at least 7 good quality tracks were considered. The selection efficiency for multihadronic events is  $(98.1 \pm 0.5)\%$ , with a background contamination smaller than 0.1%. After all cuts, a total of 3.6 million hadronic events was selected.

The selection efficiencies were estimated using samples of 2000 Monte Carlo (MC) events simulating each of the processes (see Fig. 2):

$$Z^0 \rightarrow J/\psi c\bar{c}, Z^0 \rightarrow J/\psi q\bar{q}gg, Z^0 \rightarrow J/\psi gg, Z^0 \rightarrow J/\psi q\bar{q} \text{ and } Z^0 \rightarrow J/\psi g,$$

with the subsequent decay  $J/\psi \rightarrow \ell^+\ell^-$ . In all these processes, the partons were generated using the differential cross-sections provided in [10, 11, 12, 13]. In the first three processes,  $J/\psi$  mesons are produced in a ‘colour-singlet’ state and in the last two processes, in a ‘colour-octet’ state<sup>1</sup>. Since ‘colour-octet’ states recombine into colour-singlet states by soft gluon emission, some extra energy is expected around ‘colour-octet’ states. This extra energy has been neglected in the simulation, but is taken into account later in the discussion of systematic uncertainties. A sample of 50 000 Monte Carlo events containing the decay chain  $Z^0 \rightarrow b\bar{b} \rightarrow J/\psi + X$ , and the subsequent decay  $J/\psi \rightarrow \ell^+\ell^-$ , was used to estimate the background to prompt  $J/\psi$  production from b-hadron decays. This sample was generated using the JETSET 7.4 MC program [20]. Another background source originates from four-fermion events, namely from the process  $e^+e^- \rightarrow q\bar{q} \ell^+\ell^-$ , where the  $\ell^+\ell^-$  pair results mainly from a virtual photon emission. This four-fermion background was estimated using the FERMISV generator [21]. The simulated four-fermion event sample of 20 000 events was equivalent to 20 times the expected sample in the OPAL data. For all MC samples, the parton shower and hadronisation processes were simulated using the JETSET model, with parameter settings as described in [22]. All these samples were processed using the complete OPAL detector simulation program [23].

The lepton identification and  $J/\psi$  selection requirements were the same as in [4], and are summarised below. Lepton candidates were required to satisfy the following acceptance cuts:  $p > 2 \text{ GeV}/c$ , where  $p$  is the track momentum, and  $|\cos\theta| < 0.90$ . In order to ensure a reliable calculation of the lepton pair invariant mass, an accurate polar angle measurement ( $z$  chamber association for barrel tracks, and constraint to the point where the track leaves the jet chamber in the case of forward tracks) was required for all lepton tracks.  $J/\psi$  candidates were selected by demanding two electron or two muon tracks of opposite charge, with an opening angle smaller than  $60^\circ$  and with invariant mass<sup>2</sup> in the range  $2.9\text{--}3.3 \text{ GeV}/c^2$ .

The lepton pair invariant mass distribution obtained after all preceding selection cuts (except the mass cut) is displayed in Fig. 3. The total number of  $J/\psi$  candidates in the mass range  $2.9\text{--}3.3 \text{ GeV}/c^2$  is 741. The fake  $J/\psi$  background can be obtained by counting the number of opposite-sign lepton pairs consisting of an electron and a muon ( $e^\pm\mu^\mp$ ). As discussed in [4], these lepton combinations provide a measurement of the background with a systematic error of 5%. The background calculated in this way amounts to  $230 \pm 18$  events, where the error includes both statistical and systematic contributions. The background-subtracted number of  $J/\psi$  mesons in the data sample is  $N_{J/\psi} = 511 \pm 18$ , where the error results from the background subtraction.

### 4 Selection of prompt $J/\psi$ candidates

Most of the  $J/\psi$  candidates originate from b-hadron decays and are expected to be surrounded by other b-quark decay products and by particles created in the b-quark fragmentation process. Prompt

<sup>1</sup>The colour-octet contribution to the process  $Z^0 \rightarrow J/\psi c\bar{c}$  is negligible.

<sup>2</sup>The invariant mass resolution for muon pairs is approximately  $60 \text{ MeV}/c^2$ . For electron pairs, the distribution shows a radiative tail towards low values.

$J/\psi$  mesons are expected to be rather isolated, although the degree of isolation is model dependent (see discussion below). In addition,  $J/\psi$  mesons from b-hadron decays carry the lifetime information of the parent b-hadron, whereas prompt  $J/\psi$  are expected to originate in the primary event vertex. Based on these considerations, the separation of prompt  $J/\psi$  candidates is performed with the help of the following variables:

- The ‘isolation energy’,  $E_{\text{isol}}$ . This energy is defined as the extra energy (sum of track momenta and energy of electromagnetic clusters not associated to tracks), contained within a cone of half-angle  $30^\circ$  around the direction of the reconstructed  $J/\psi$ .
- The ‘decay length significance’,  $L/\sigma_L$ , of the lepton pair. The decay length  $L$  is obtained as the distance in the  $x - y$  plane between the estimated event vertex position and the dilepton decay vertex, using the direction of the reconstructed  $J/\psi$  as a constraint (a more detailed description can be found in [24]). The error in  $L$ ,  $\sigma_L$ , is estimated from the track parameter errors and the uncertainty in the position of the event vertex.

The  $E_{\text{isol}}$  distribution for all  $J/\psi$  candidates is displayed in Fig. 4, together with the distributions for the fake  $J/\psi$  background and for simulated  $J/\psi$  mesons originating in b-hadron decays. The MC sample is normalised to the number of  $J/\psi$  mesons found in the data after demanding  $L/\sigma_L > 2$ , in order to ensure that the  $J/\psi$  sample originates in b-hadron decays. An excess of events is observed at small values of  $E_{\text{isol}}$ . Furthermore, this excess of events is enhanced at small values of  $L/\sigma_L$  (namely  $|L|/\sigma_L < 4$ ), as shown in Fig. 5. No excess is observed, on the contrary, in the b-decay enriched sample obtained for  $L/\sigma_L > 4$  (see Fig. 6). The  $L/\sigma_L$  distribution for  $J/\psi$  candidates satisfying  $E_{\text{isol}} > 4$  GeV is displayed in Fig. 7. As shown by Fig. 6 and 7, the MC is able to reproduce, in the regions of interest for this analysis, both the  $E_{\text{isol}}$  and  $L/\sigma_L$  distributions for b-decay dominated samples.

In the following, prompt  $J/\psi$  candidates are selected using the two additional cuts:

$$E_{\text{isol}} < 4 \text{ GeV} \quad \text{and} \quad |L|/\sigma_L < 4 .$$

The invariant mass distribution after these cuts (except the mass cut) is displayed in Fig. 8. This distribution shows a peak at the position of the  $J/\psi$  mass. Therefore the observed excess of events is not due to a source like four-fermion processes, since this source produces mainly a non-resonant background (see below). The total number of prompt  $J/\psi$  candidates in the mass range 2.9–3.3 GeV/ $c^2$  is  $N_{\text{cand}} = 24$ . The background in this mass range can originate from the following sources:

- Fake  $J/\psi$  candidates, determined from  $e^\pm \mu^\mp$  combinations. This background amounts to  $2.0 \pm 1.4$  events, the error being mainly statistical (the systematic error is of the order of 5%).
- Lepton pairs from four-fermion events. This background has been calculated using the four-fermion simulated sample and amounts to  $1.6 \pm 0.4$  events, the error being again mainly statistical (the theoretical error is of the order of 10% as discussed in [25]). This background value includes a small contribution of 0.2 events from resonant  $J/\psi$  production.
- Real  $J/\psi$  candidates originating in b-hadron decays. This background has been calculated using the b-decay simulated sample and amounts to  $7.2 \pm 1.1$  events. The various contributions to the total error are detailed in Table 1. The  $J/\psi$  momentum spectrum in b-decays (at rest) has been reweighted to match the distribution measured by CLEO [26]. The difference between this spectrum and the spectrum obtained with JETSET is used to calculate the systematic error for this background source. The MC events were generated using the Peterson fragmentation function for b-quarks [27], with an average energy of the primary b-hadron, scaled by the beam energy, of  $\langle x_E \rangle_b = 0.713 \pm 0.012$ , as in [4]. The inclusive b-hadron lifetime  $\tau_b = 1.54 \pm 0.02$  ps [28] has also been used in the event simulation. The experimental errors on these two quantities have been used to calculate the corresponding systematic errors for the background. Finally a variation of track parameter resolutions as in [4] has been performed to estimate the uncertainties in the modelling by the MC of the  $E_{\text{isol}}$  and  $L/\sigma_L$  quantities.

The total background is therefore  $N_{\text{bkg}} = 10.8 \pm 1.8$ , and the background-subtracted number of prompt  $J/\psi$  candidates is:

$$N_{\text{prompt}} = N_{\text{cand}} - N_{\text{bkg}} = 13.2 \pm 4.9 \pm 1.8,$$

where the first error is statistical and the second results from the background uncertainty. The probability that the background fluctuates to the observed signal of 24 events is  $2 \cdot 10^{-4}$ .

Error source	Events
normalisation error	0.2
$J/\psi$ spectrum in b-decays	0.8
b-quark fragmentation	0.4
b-quark lifetime	0.1
track parameter resolution	0.2
MC statistics	0.6
Total background uncertainty	1.1

Table 1: *Contributions to the background uncertainty for  $J/\psi$  originating from b-hadron decays.*

## 5 Inclusive branching ratio

The fraction of prompt  $J/\psi$  events in  $Z^0$  decays is calculated as follows:

$$\frac{Br(Z^0 \rightarrow \text{prompt } J/\psi + X)}{Br(Z^0 \rightarrow J/\psi + X)} = \frac{N_{\text{prompt}}}{N_{J/\psi}} \cdot \frac{\epsilon_{J/\psi}}{\epsilon_{\text{prompt}}}$$

where  $\epsilon_{J/\psi}$  is the efficiency to select all  $J/\psi$  candidates, and  $\epsilon_{\text{prompt}}$  is the efficiency to select prompt  $J/\psi$  candidates. The efficiency  $\epsilon_{J/\psi}$ , calculated using the b-decay MC, is  $\epsilon_{J/\psi} = 0.230 \pm 0.002$ , where the error is statistical. The small proportion of prompt  $J/\psi$  events in the total  $J/\psi$  sample introduces a negligible correction to  $\epsilon_{J/\psi}$ . The  $\epsilon_{\text{prompt}}$  efficiency depends very significantly on the production process, as can be seen in Table 2. This dependence is introduced in particular by the isolation cut (see also Fig. 9). For each process the theoretically predicted branching ratio is reported in Table 2. The average efficiency, obtained by weighting individual efficiencies according to the theoretically expected rates, is  $\epsilon_{\text{prompt}} = 0.146 \pm 0.008$ , where the error is statistical. Taking into account that a prompt  $J/\psi$  may originate also from cascade decays, and that direct  $J/\psi$ ,  $\psi'$  and  $\chi_c$  states are produced with relative abundances 0.5:0.2:0.3 [13], this efficiency is further reduced to  $\epsilon_{\text{prompt}} = 0.129 \pm 0.007$ . This value is used below to calculate the  $Z^0$  branching ratio to prompt  $J/\psi$  events.

The following systematic uncertainties have been considered (see Table 3):

- The uncertainties on  $N_{J/\psi}$  and  $N_{\text{prompt}}$  due to the background subtraction were determined as described above.
- Most of the systematic uncertainties on the efficiencies cancel in the ratio  $\epsilon_{J/\psi}/\epsilon_{\text{prompt}}$ . The uncertainty on  $\epsilon_{\text{prompt}}$  due to the extra cuts on  $E_{\text{isol}}$  and  $L/\sigma_L$  was determined by varying the track parameter resolutions, as in [4]. There is in addition an uncertainty related to the MC modelling of the  $E_{\text{isol}}$  energy for colour-octet models, due to soft gluon emission. This uncertainty can be estimated by comparing the efficiency for the processes  $Z^0 \rightarrow J/\psi q\bar{q}$  (with no gluon emission) and  $Z^0 \rightarrow J/\psi q\bar{q}g$  (with the emission of two hard gluons), and is included in the model uncertainty discussed below.

Production process	Efficiency no isolation cut	Efficiency isolation cut	$Br(Z^0 \rightarrow \text{prompt } J/\psi + X)$ expected
$Z^0 \rightarrow J/\psi \ c\bar{c}$	$0.262 \pm 0.011$	$0.084 \pm 0.006$	$0.8 \cdot 10^{-4}$ [13]
$Z^0 \rightarrow J/\psi \ q\bar{q}gg$	$0.203 \pm 0.010$	$0.104 \pm 0.007$	$0.2 \cdot 10^{-4}$ [11]
$Z^0 \rightarrow J/\psi \ gg$	$0.215 \pm 0.010$	$0.148 \pm 0.009$	$0.5 \cdot 10^{-6}$ [12]
$Z^0 \rightarrow J/\psi \ q\bar{q}$	$0.221 \pm 0.011$	$0.174 \pm 0.009$	$1.9 \cdot 10^{-4}$ [13]
$Z^0 \rightarrow J/\psi \ g$	$0.273 \pm 0.012$	$0.271 \pm 0.012$	$1.6 \cdot 10^{-7}$ [13]

Table 2: Monte Carlo calculation of  $J/\psi$  selection efficiencies for the various prompt  $J/\psi$  production models. The last column gives the theoretical branching ratio for each process. The errors are statistical.

- The prompt  $J/\psi$  selection efficiency has been calculated assuming that  $J/\psi$  mesons decay isotropically. In order to account for the unknown  $J/\psi$  polarization, the efficiency has been recalculated assuming that the angular distribution of leptons from  $J/\psi$  decays is proportional to  $1 + \cos^2 \theta^*$ , where  $\theta^*$  is the emission angle in the  $J/\psi$  rest frame with respect to the  $J/\psi$  direction in the laboratory frame.
- As mentioned before, the efficiency  $\epsilon_{\text{prompt}}$  is reduced if the  $J/\psi$  originates in cascade decays from  $\psi'$  and  $\chi_c$  states. The correction of 13.5% introduced before to account for this effect is included as a systematic uncertainty.

The stability of the result was checked by varying the  $E_{\text{isol}}$  cut between 3 and 5 GeV. It was found that this variation does not contribute to any systematic shift in the result.

Error source	Contribution
background to $N_{\text{prompt}}$	13.6 %
background to $N_{J/\psi}$	3.5 %
efficiency ratio	7.2 %
polarization	9.5 %
cascade decays	13.5 %
MC statistics	5.5 %
Total systematic error	23.5 %

Table 3: Summary of systematic uncertainties on the fraction of prompt  $J/\psi$  events in  $Z^0$  decays.

Taking into account the statistical and systematic uncertainty, the fraction of prompt  $J/\psi$  events in  $Z^0$  decays is:

$$\frac{Br(Z^0 \rightarrow \text{prompt } J/\psi + X)}{Br(Z^0 \rightarrow J/\psi + X)} = (4.6 \pm 1.7 \pm 1.1)\%.$$

The momentum distribution of prompt  $J/\psi$  candidates is displayed in Fig. 10. This distribution is compatible with all models of prompt  $J/\psi$  production except  $Z^0 \rightarrow J/\psi \ g$ . In this last model, the momentum, scaled by the beam energy, is expected to exceed 0.95 for 90% of the candidates. Since no event is observed in this momentum region, an upper limit of 10% (at 90% CL) can be obtained for the contribution of this process to the total prompt  $J/\psi$  signal.

As explained before, the average efficiency  $\epsilon_{\text{prompt}}$  depends on the theoretically expected rates for each of the production processes, but these calculated rates have large uncertainties. An additional error is therefore included to account for these theoretical uncertainties. This error is calculated as

the r.m.s. spread of the efficiencies for the various production models (see Table 2) and amounts to 27.5%. The  $Z^0 \rightarrow J/\psi$  g process has been excluded from the calculation, since both the theoretical branching ratio and the momentum distribution of prompt candidates indicate that its contribution to the total signal is likely to be small.

Taking into account all uncertainties, the fraction of prompt  $J/\psi$  events in  $Z^0$  decays is:

$$\frac{Br(Z^0 \rightarrow \text{prompt } J/\psi + X)}{Br(Z^0 \rightarrow J/\psi + X)} = (4.6 \pm 1.7 \pm 1.1 \pm 1.3)\%,$$

where the first error is statistical, the second systematic, and the third error accounts for model uncertainties. Using the measurement from [4]  $Br(Z^0 \rightarrow J/\psi + X) = (3.9 \pm 0.2 \pm 0.3) \cdot 10^{-3}$ , the following inclusive branching ratio is obtained:

$$Br(Z^0 \rightarrow \text{prompt } J/\psi + X) = (1.8 \pm 0.7 \pm 0.5 \pm 0.5) \cdot 10^{-4}.$$

This branching ratio is in agreement with the theoretical expectation of  $2.9 \cdot 10^{-4}$ , obtained by adding together all production mechanisms. If ‘colour-singlet’ models alone are considered, the measured branching ratio would be  $Br(Z^0 \rightarrow \text{prompt } J/\psi + X) = (2.6 \pm 0.9 \pm 0.4 \pm 0.7) \cdot 10^{-4}$ , to be compared with the theoretical expectation of  $1.0 \cdot 10^{-4}$ . The experimental measurement does not exclude the hypothesis that the prompt  $J/\psi$  signal can be explained by ‘colour-singlet’ processes alone. This result is also compatible with the upper limit of  $4 \cdot 10^{-4}$  obtained by DELPHI for colour-singlet processes [6].

## 6 Summary

The production of prompt  $J/\psi$  mesons in hadronic  $Z^0$  decays has been studied using a sample of 3.6 million hadronic  $Z^0$  decays. A total of 511  $J/\psi$  mesons are identified from their decays into  $e^+e^-$  and  $\mu^+\mu^-$  pairs. Prompt  $J/\psi$  candidates are selected by requiring that the  $J/\psi$  be isolated and not significantly displaced from the event vertex. The number of prompt candidates is 24, with an estimated background of  $10.8 \pm 1.8$  events. The probability that the background fluctuates to the observed number of 24 events is  $2 \cdot 10^{-4}$ . Assuming that the dominant production mechanism is gluon fragmentation into ‘colour-octet’  $J/\psi$  states, the following measurement of the fraction of prompt  $J/\psi$  events in the total sample is obtained:

$$\frac{Br(Z^0 \rightarrow \text{prompt } J/\psi + X)}{Br(Z^0 \rightarrow J/\psi + X)} = (4.6 \pm 1.7 \pm 1.1 \pm 1.3)\%,$$

corresponding to an inclusive branching ratio of

$$Br(Z^0 \rightarrow \text{prompt } J/\psi + X) = (1.8 \pm 0.7 \pm 0.5 \pm 0.5) \cdot 10^{-4}.$$

In both cases, the first error is statistical, the second systematic and the third error is obtained after consideration of other possible production mechanisms.

## References

- [1] ALEPH Collab., D.Buskulic et al., Phys.Lett. **B295** (1992) 396.
- [2] L3 Collab., O.Adriani et al., Phys.Lett. **B317** (1993) 467.
- [3] DELPHI Collab., P.Abreu et al., Phys.Lett. **B341** (1994) 109.
- [4] OPAL Collab., G.Alexander et al., *J/ψ and ψ′ production in hadronic Z<sup>0</sup> decays*, CERN-PPE/95-153, to be published in Z. Phys. **C**.

- [5] OPAL Collab., G.Alexander et al., *Observation of  $\Upsilon$  production in hadronic  $Z^0$  decays*, CERN-PPE/95-181, to be published in Phys.Lett. **B**.
- [6] DELPHI Collab., P.Abreu et al., *Search for promptly produced heavy quarkonium states in hadronic  $Z$  decays*, CERN-PPE/95-145, to be published in Z. Phys. **C**.
- [7] M.Cacciari et al., Phys. Rev. Lett. **73** (1994) 1586;  
M.Cacciari et al., Phys. Lett. **B356** (1995) 553.
- [8] P.Cho and A.Leibovich, Phys. Rev. **D53** (1996) 150.
- [9] P.Cho and A.Leibovich, *Color-Octet quarkonia production II*, CALT 68-2026.
- [10] E.Braaten, K.Cheung, T.C.Yuan, Phys. Rev. **D48** (1993) 4230;  
V.Barger, K.Cheung, and W.Y.Keung, Phys. Rev. **D41** (1990) 1541.
- [11] E.Braaten, T.C.Yuan, Phys. Rev. Lett. **71** (1993) 1673;  
K.Hagiwara, et al., Phys. Lett. **B267** (1991) 527, Erratum: Phys. Lett. **B316** (1993) 631.
- [12] J.H.Kühn and H.Schneider, Z. Phys. **C11** (1981) 263;  
W.Y.Keung, Phys. Rev. **D23** (1981) 2072.
- [13] P.Cho, Phys. Lett. **B368** (1996) 171.  
The branching ratio  $Br(Z^0 \rightarrow J/\psi q\bar{q})$  quoted in this paper is  $3.3 \cdot 10^{-4}$ . This value is obtained using the results from [8]. If the more recent results from [9] are used instead, this branching ratio becomes  $1.9 \cdot 10^{-4}$ .
- [14] K.Cheung, W.Y. Keung and T.C.Yuan, *Colour-Octet Quarkonium Production at the  $Z$  Pole*, FERMILAB-PUB-95/300-T.
- [15] OPAL Collab., K.Ahmet et al., Nucl. Instrum. and Meth. **A305** (1991) 275.
- [16] P.Allport et al., Nucl. Instrum. and Meth. **A324** (1993) 34;  
P.Allport et al., Nucl. Instrum. and Meth. **A346** (1994) 476.
- [17] M.Hauschild et al., Nucl. Instrum. and Meth. **A314** (1992) 74.
- [18] OPAL Collab., G.Alexander et al., Z. Phys. **C52** (1991) 175.
- [19] OPAL Collab., P.Acton et al., Z. Phys. **C58** (1993) 523.
- [20] T.Sjöstrand, Comp. Phys. Comm. **82** (1994) 74;  
T.Sjöstrand, JETSET 7.4 Manual, CERN-TH.7112/93.
- [21] J.M.Hilgart, R.Kleiss and F.Le Diberder, Comp. Phys. Comm. **75** (1993) 191.
- [22] OPAL Collab., G.Alexander et al., *A Comparison of  $b$  and  $uds$  quark jets to gluon jets*, CERN-PPE/95-126, to be published in Z. Phys. **C**.
- [23] J.Allison et al., Nucl. Instrum. and Meth. **A317** (1991) 47.
- [24] OPAL Collab., R.Akers et al., Z. Phys. **C65** (1995) 17.
- [25] L3 Collab., A.Adam et al., Phys. Lett. **B321** (1994) 283;  
ALEPH Collab., D.Buskulic et al., Z. Phys. **C66** (1995) 3.
- [26] CLEO Collab., R.Balest et al., Phys.Rev. **D52** (1995) 2661.
- [27] C.Peterson et al., Phys.Rev. **D27** (1983) 105.
- [28] L.Montanet et al., Review of Particle Properties, Phys. Rev. **D50** (1994) 1173.



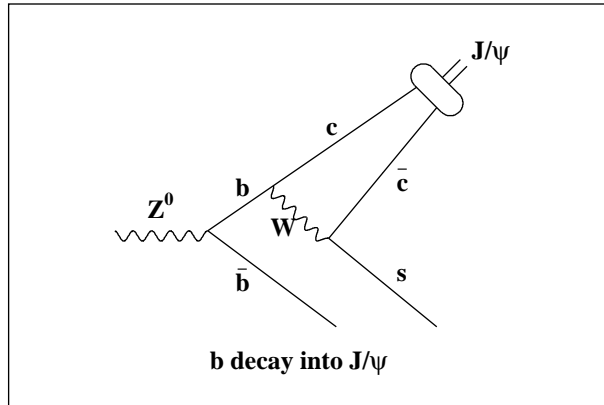


Figure 1: Feynman diagram for  $J/\psi$  production in a b-quark decay.

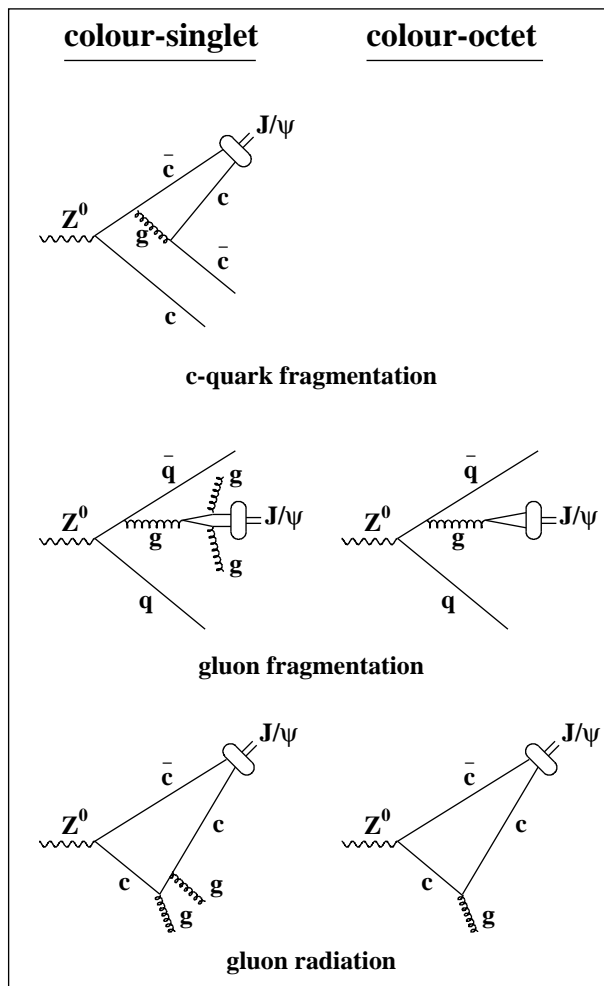


Figure 2: Feynman diagrams for various prompt  $J/\psi$  ‘colour-singlet’ ( $Z^0 \rightarrow J/\psi c\bar{c}$ ,  $Z^0 \rightarrow J/\psi q\bar{q}gg$  and  $Z^0 \rightarrow J/\psi gg$ ) and ‘colour-octet’ ( $Z^0 \rightarrow J/\psi q\bar{q}$  and  $Z^0 \rightarrow J/\psi g$ ) production processes.

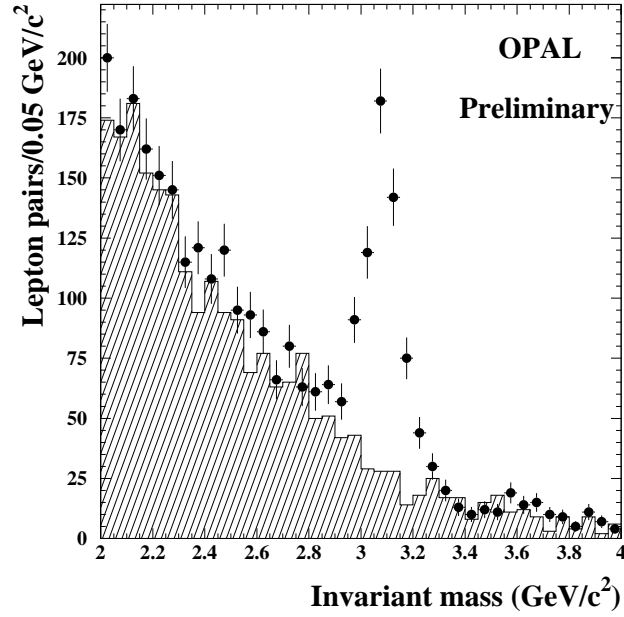


Figure 3: Invariant mass distribution of  $e^+e^-$  and  $\mu^+\mu^-$  pairs. The shaded histogram of  $e^\pm\mu^\mp$  pairs used to calculate the fake  $J/\psi$  background is superimposed.

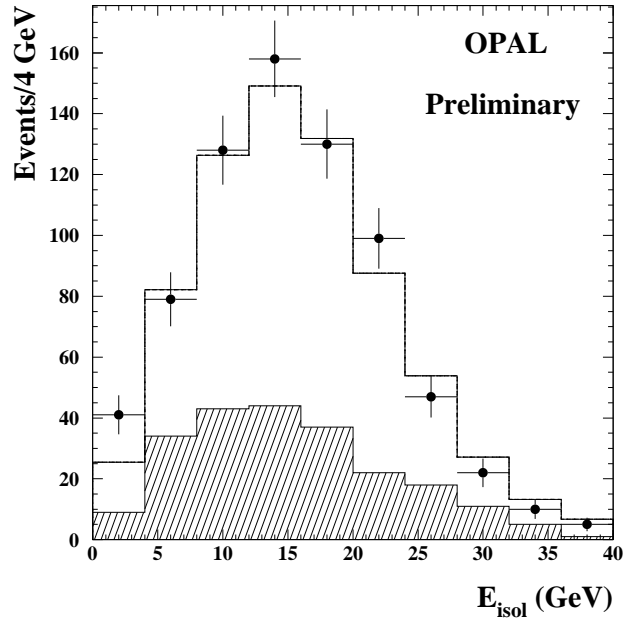


Figure 4:  $E_{\text{isol}}$  distribution for all  $J/\psi$  candidates. The shaded histogram represents the  $E_{\text{isol}}$  distribution for  $e^\pm\mu^\mp$  pairs. The solid line represents the expected distribution for b-quark decays, added to the fake  $J/\psi$  background.

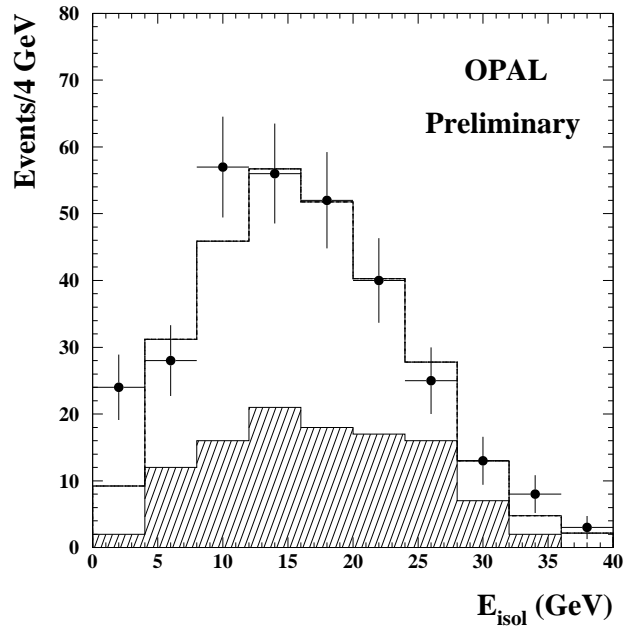


Figure 5:  $E_{\text{isol}}$  distribution for  $J/\psi$  candidates satisfying  $|L|/\sigma_L < 4$ . The shaded histogram represents the  $E_{\text{isol}}$  distribution for  $e^\pm\mu^\mp$  pairs. The solid line represents the expected distribution for b-quark decays, added to the fake  $J/\psi$  background.

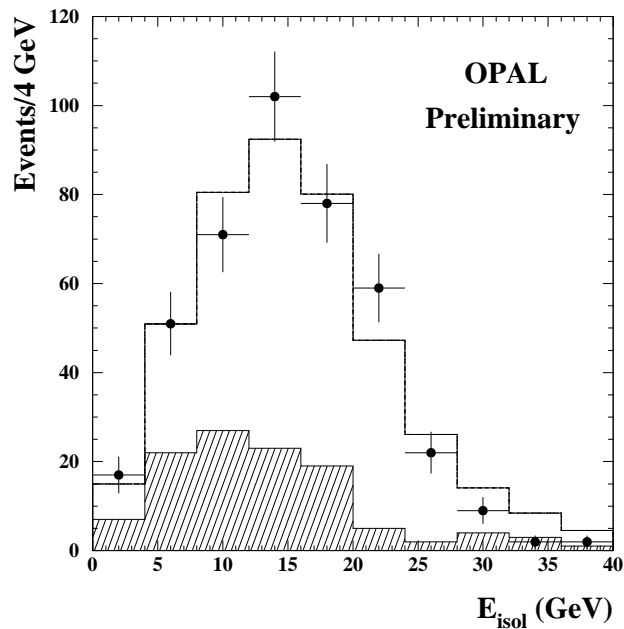


Figure 6:  $E_{\text{isol}}$  distribution for  $J/\psi$  candidates satisfying  $L/\sigma_L > 4$ . The shaded histogram represents the  $E_{\text{isol}}$  distribution for  $e^\pm\mu^\mp$  pairs. The solid line represents the expected distribution for b-quark decays, added to the fake  $J/\psi$  background.

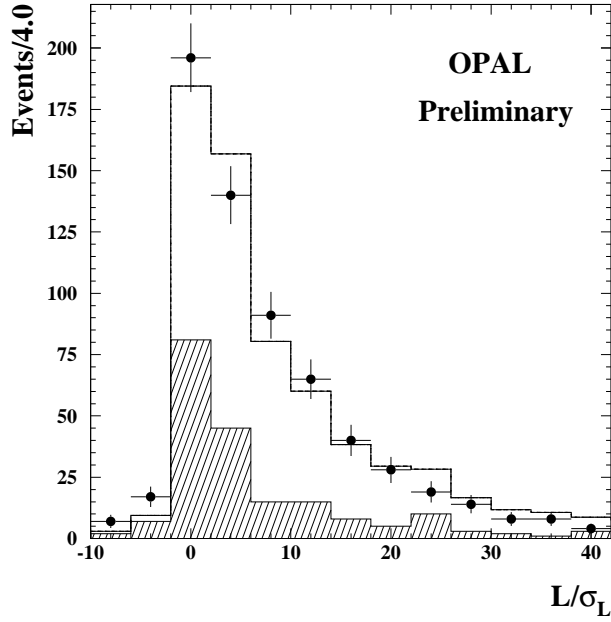


Figure 7:  $L/\sigma_L$  distribution for  $J/\psi$  candidates satisfying  $E_{\text{isol}} > 4$  GeV. The shaded histogram represents the  $L/\sigma_L$  distribution for  $e^\pm\mu^\mp$  pairs. The solid line represents the expected distribution for b-quark decays, added to the fake  $J/\psi$  background.

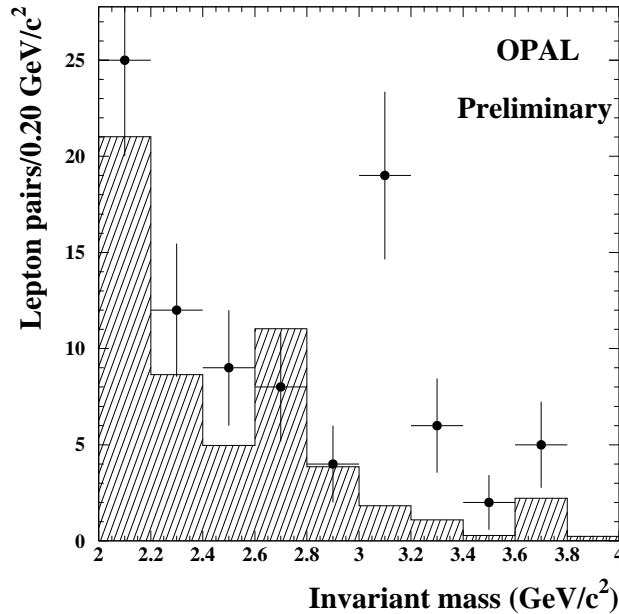


Figure 8: Invariant mass distribution of  $e^+e^-$  and  $\mu^+\mu^-$  pairs after all selection cuts. The shaded histogram includes  $e^\pm\mu^\mp$  pairs used to calculate the fake  $J/\psi$  background and the four-fermion background.

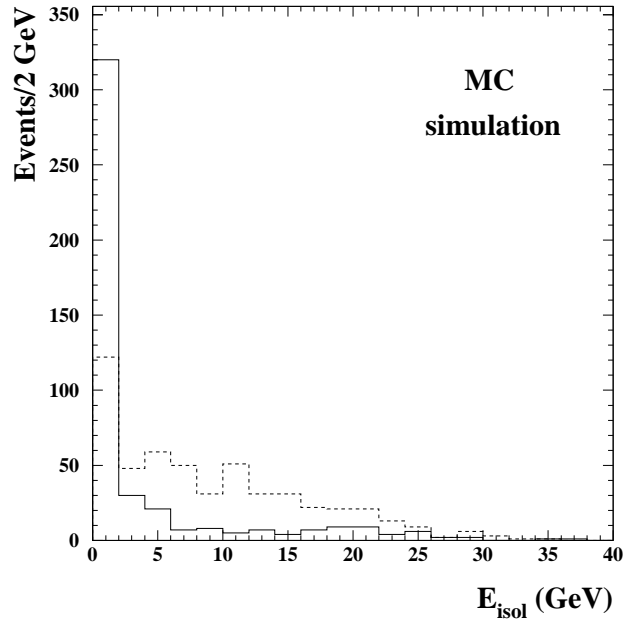


Figure 9: Simulated  $E_{\text{isol}}$  distribution for  $J/\psi$  mesons produced according to the processes  $Z^0 \rightarrow J/\psi q\bar{q}$  (solid line) and  $Z^0 \rightarrow J/\psi c\bar{c}$  (dashed line). According to the theoretical calculations reported in Table 2, these two processes are dominant.

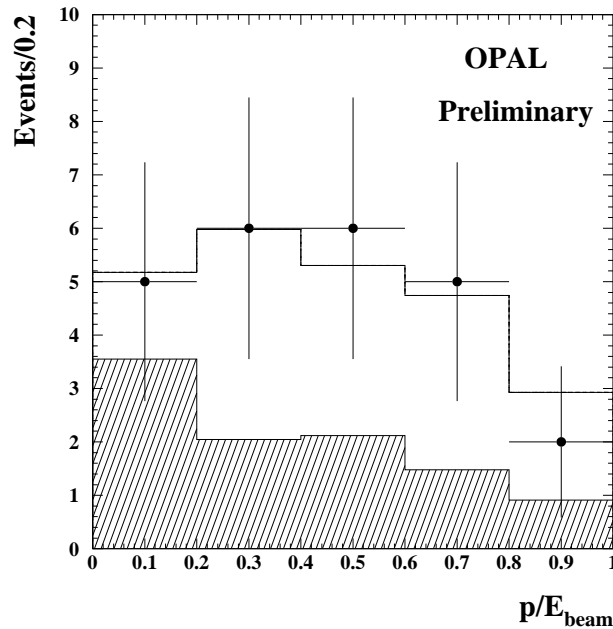


Figure 10: Momentum distribution of prompt  $J/\psi$  candidates. The shaded histogram includes all background sources and the solid line represents the background added to the simulated prompt  $J/\psi$  distribution.